Aalborg Universitet

Aalborg Universitet

TS Fuzzy Model-Based Controller Design for a Class of Nonlinear Systems Including Nonsmooth Functions

Vafamand, Navid; Asemani, Mohammad Hassan; Khayatiyan, Alireza ; Khooban, Mohammad Hassan; Dragicevic, Tomislav

TS Fuzzy Model-Based Controller Design for a Class of Nonlinear Systems Including Nonsmooth Functions

Navid Vafamand, Mohammad Hassan Asemani[ID], Alireza Khayatiyan,
Mohammad Hassan Khooban[ID], and Tomislav Dragičević

Abstract—This paper proposes a novel robust controller design for a class of nonlinear systems including hard nonlinearity functions. The proposed approach is based on Takagi–Sugeno (TS) fuzzy modeling, nonquadratic Lyapunov function, and nonparallel distributed compensation scheme. In this paper, a novel TS modeling of the nonlinear dynamics with signum functions is proposed. This model can exactly represent the original nonlinear system with hard nonlinearity while the discontinuous signum functions are not approximated. Based on the bounded-input-bounded-output stability scheme and L_1 performance criterion, new robust controller design conditions in terms of linear matrix inequalities are derived. Three practical case studies, electric power steering system, a helicopter model and servo-mechanical system, are presented to demonstrate the importance of such class of nonlinear systems comprising signum function. Furthermore, to show the superiorities of the proposed approach, it is applied to these systems; and, the experimental real-time hardware-in-the-loop results are compared with the published literature with the same topic.

Index Terms—Electric power steering (EPS) system, hardware-in-the-loop (HIL), helicopter system, nonsmooth dynamical equations, robust L_1 controller, servo-system, signum function, Takagi–Sugeno (TS) fuzzy model.

I. INTRODUCTION

SIGNUM function is a discontinues hard nonlinearity term that exists in the dynamics of many physical systems such as electrical circuits, mechanical systems and robots [1]–[3]. Signum functions can model different physical and practical phenomena such as friction force that is modeled as a function of the velocity [1], spring force that is a function of the position [4] and backlash which is formulated by linear and signum functions. The signum function has appeared in chaotic systems [5], electromechanical relays and thyristor circuits [6]. The occurrence of the signum function can lead to chattering in the physical systems, due to its discontinues nature [1], [6].

Controlling the class of nonlinear systems comprising the signum function is difficult. Different nonlinear controllers are proposed for this class of nonlinear systems [7]–[11]. In [7], a motion control is presented for robots with nonlinear friction force modeled by signum function. The controller is designed such that the soft nonlinearities are compensated and then, the hard nonlinearities are controlled. In [12], an adaptive control of a joint robot, that the signum function appears in its dynamic, is studied. This method does not need the exact representation of the model and the system parameters including the coefficients of the signum functions can be unknown. In [13], an adaptive controller is proposed for servo actuator comprising the signum function modeling friction forces. However, introducing update law for parameter estimation of the signum parameters complicates the real implantation of the adaptive controllers [12], [13]. In [9], a robust time delay controller is designed for a smart unmanned aerial vehicle (SUAV). Dry friction is considered in nonlinear dynamic of the SUAV. Based on the error vector, the controller stabilizes the error dynamics to achieve a tracking control problem. However, the approach of [9] suffers from the highly oscillating control input signal. In [10], a local H_∞ controller is designed for a servo-system with a flexible shaft involving backlash, coulomb and viscous friction forces. Two dynamical Riccati equations should be solved for a linearized nonsmooth system and based on the simplified linearized model; a linear controller is designed to guarantee the local stabilization of the original system. In [14], a robust switching controller for a two mass system with backlash is proposed. The system dynamic is divided into three modes. For each of these modes a linear controller and backlash compensator is designed. However, the control law must frequently and rapidly switches among these modes with the backlash amplitude decreases. In [11], a sum of square approach is proposed for pitch control of helicopter system. There exists a signum function in the nonlinear dynamic of the helicopter. First, the nonlinear terms are approximated by polynomial functions in several regions. Then, for each region, a polynomial controller is designed based on the semi-definite techniques [15]. However, to achieve a desirable closed-loop performance, higher number of region should be considered which complicates the controller design procedure.

This article has been accepted for inclusion in a future issue of this journal. Content is final as presented, with the exception of pagination.

2

IEEE TRANSACTIONS ON SYSTEMS, MAN, AND CYBERNETICS: SYSTEMS

Recently, Takagi–Sugeno (TS) model-based control has been widely used for complex nonlinear systems [16]–[20]. Parallel distributed compensation (PDC) and non-PDC control structures provide systematic approaches to accomplish the stabilization and performance issues for such TS models in terms of linear matrix inequalities (LMIs) [21]–[23]. Most of the existing TS-based control designs are presented for continuous dynamics. To the best knowledge of the authors, few TS-based literatures consider the discontinuous nonlinear dynamics such as signum functions and derive controller design conditions [24], [25].

Since, the signum function is discontinues, it cannot be exactly represented by a TS fuzzy model. Different methods have been presented for TS modeling of this function. These approaches can be classified in two categories: first, is to approximate the nonsmooth signum function with a smooth one and deriving the corresponding TS model. Second, is to directly derive a TS model based on linearization technique [24], [25]. In the first method, different smooth functions can be considered, such as sigmoid function [26], hyperbolic tangent function [27], [28], and polynomial function [29]. Then, an approximated TS model of these smooth functions can be derived via sector nonlinearity approach. In [30], by approximating a signum function by hyperbolic function, a quasilinear parameter varying model with four vertices is derived. Then, the simplified model is discretized and a controller is designed via LMI techniques. In [25], an approximated TS model of electric power steering (EPS) system is derived. Although, the system comprises three signum functions, by considering some simplifications, a two-rule TS system with time delay state-space representation is obtained. In [24], based on the simplification method given in [25], a new TS modeling of the nonlinear the EPS system is presented and PDC controller with saturation constraint is developed. In the first category, the membership functions are smooth and derivable; meanwhile the membership functions obtained based on the second category is nonderivable in general. However, both approaches provide an approximated TS model for the signum function.

In this paper, a new systematic approach for controlling a class of nonlinear dynamics with the signum function is proposed. This approach is based on the TS fuzzy model, the non-PDC controller and the NQLF. In this approach, the signum functions are not modeled by a TS representation; and, instead of asymptotic stabilization, bounded-input-bounded-output (BIBO) stability criterion is considered. Consequently, based on the L_1 performance criterion, a robust non-PDC controller is designed such that the ratio of upper bound of the signum functions with respect to the L_∞ norm of the output is attenuated to be lower than a pregiven threshold. The proposed approach has some main advantages over the existing works. Since we take the signum functions as a persistent bounded disturbance, the obtained TS model exactly represents the nonlinear dynamics comprising the signum functions, In other words, signum functions are not modeled by TS fuzzy system. Consequently, the overall TS fuzzy system with less number of fuzzy rules is obtained which relaxes the controller design conditions. As a result, a simpler TS-based controller

is constructed which comprises less number of fuzzy rules. To show the merits of the proposed approach, it is applied to EPS, helicopter, and servo systems and the results are compared with other recently published works concerning the same topic. Simulation results show that not only the BIBO stability is achieved but also the outputs of the aforementioned systems roughly converge to their equilibrium points. In addition, no chattering and oscillatory phenomena exhibit in the closed-looped nonlinear systems.

This paper is organized as follows. In Section II, the class of nonlinear systems with nonsmooth functions is described and three motivating practical EPS system, helicopter, and servo-motor systems are presented. In Section III, the L_1 performance criterion, non-PDC scheme and NQLF are studied and the main results of this paper are discussed in Section IV. In Section V, the simulation results are illustrated and compared with recent works in hand. Finally, in Section VI, the conclusion remarks are presented.

II. NONLINEAR SYSTEMS WITH NONSMOOTH FUNCTIONS

Consider the following nonlinear dynamic equation that comprises nonsmooth function:

$$\dot{x}(t) = A(x(t)) + B(x(t))u(t) + E(x(t))nsf(x(t))$$
$$y(t) = C(x(t)) \tag{1}$$

where $A(\cdot)$, $B(\cdot)$, $E(\cdot)$, and $C(\cdot)$ are nonlinear functions, $x(t) \in \mathcal{R}^{n \times 1}$ and $y(t) \in \mathcal{R}^{m \times 1}$ are the state and controlled output vectors, respectively. Furthermore, $nsf(x(t)) \in \mathcal{R}^{k \times 1}$ is a vector whose arrays are bounded nonsmooth functions (such as signum and saturation) of the system's states. We are interested in deriving TS model of the nonlinear dynamic equation (1). However, due to the discontinuity of the hard nonlinear functions such as signum function, their equivalent TS representations are not available [6]. To solve this TS modeling difficulty, we consider the following TS representation:

$$\dot{x}(t) = \sum_{i=1}^{r} h_i(z(t))\{A_i x(t) + B_i u(t) + E_i nsf(x(t))\}$$
$$y(t) = \sum_{i=1}^{r} h_i(z(t))C_i x(t) \tag{2}$$

where $z(t) \in \mathcal{R}^{p \times 1}$ is a vector whose elements are bounded, smooth, and functions of the states and $h_i(z(t))$ are the normalized membership functions which satisfy the convex sum property

$$\sum_{i=1}^{r} h_i(z(t)) = 1. \tag{3}$$

As it can be seen in (2), the signum functions are explicitly appeared in the TS representation. To show the necessity and applicability of the given structure in (1), in the following, we will present some motivating practical examples that can be restated as the nonlinear dynamic equation (1) and the TS model (2). The two first examples include dry and coulomb friction forces. Meanwhile, the third system involves backlash property.

This article has been accepted for inclusion in a future issue of this journal. Content is final as presented, with the exception of pagination.

VAFAMAND *et al.*: TS FUZZY MODEL-BASED CONTROLLER DESIGN FOR CLASS OF NONLINEAR SYSTEMS
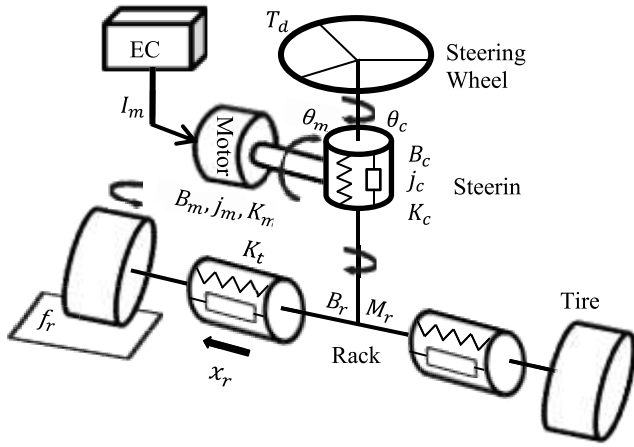
3

Fig. 1. Diagram of the EPS system.

A. EPS System

The conventional hydraulic steering systems have been replaced by the EPS Systems due to their modularity, tenability of steering feel, and environmental friendliness [24]. The nonlinear dynamic model of the EPS system drawn in Fig. 1 is given by the relation between mechanical steering system, a brush-type direct current motor and tire/road contact forces [25]

$$
\begin{cases}
\dot\theta_c = w_c \\
\dot w_c = \frac{1}{j_c}(T_d - T_c - B_c w_c - F_c \mathrm{sgn}(w_c)) \\
\dot\theta_m = w_m \\
\dot w_m = \frac{1}{j_m}(T_a - T_m - B_m w_m - F_m \mathrm{sgn}(w_m)) \\
\dot x_r = v_r \\
\dot v_r = \frac{\frac{T_c + G_G T_m}{r_p} - K_t x_r - f_r - B_r v_r - F_r \mathrm{sgn}(v_r)}{M_r}
\end{cases}
\tag{4}
$$

where θ_c and w_c are the steering hand wheel angle and velocity, respectively, θ_m and w_m are the motor angular position and velocity, respectively, and x_r and v_r are the rack position and velocity, respectively. In addition, j_c is the steering column moment of inertia, T_d is torque on the steering wheel enforced by the driver, T_c is the steering torque, B_c is the steering column viscous damping, and F_c is the steering column friction. Also, j_m is the motor moment of inertia, T_a is the effective assisting torque, T_m is the servo force, B_m is the motor damping, and F_m is the motor friction. Furthermore, M_r is the rack and wheel assembly mass, G_G is the motor gear ratio, r_p is the radius of the pinion, k_t is the tire spring rate, B_r is the rack damping, and f_r is the rack force. In the dynamic of the EPS system (4), the effective assisting torque, steering torque force, and servo force are derived as [24]

$$
\begin{cases}
T_a = K_a I_m \\
T_c = K_c\left(\theta_c - \frac{x_r}{r_p}\right) \\
T_m = K_m\left(\theta_m - \frac{G_G x_r}{r_p}\right)
\end{cases}
\tag{5}
$$

where K_a is the motor torque constant, I_m is the armature current, K_c is the steering column stiffness, and K_m is the motor torsional stiffness. The rack force f_r can be derived

based on the vehicle model with single track, so-called bicycle model

$$
f_r = \frac{T_P C_f}{r_p}\left\{\delta_f - \beta - \frac{l_f}{V}\gamma\right\}
\tag{6}
$$

where $\delta_f = \theta_c/G_{sc}$ is the front steer angle, G_{sc} is the steering system ratio, T_P is the caster trail, C_f is the cornering stiffness coefficient, l_f is the chassis length of front, and V is speed of the vehicle which is assumed to be constant [25]. In addition, β and γ denote the side slip angle and the yaw rate, respectively. By considering small angle approximations, one has [25]

$$
\begin{cases}
\dot\beta = \dfrac{-(C_f+C_r)\beta - \left(MV - \frac{1}{V}(l_f C_f - l_r C_r)\right)\gamma + C_f \delta_f}{MV} \\[2ex]
\dot\gamma = \dfrac{-(l_f C_f - l_r C_r)\beta - \frac{1}{V}\left(l_f^2 C_f + l_r^2 C_r\right)\gamma + l_f C_f \delta_f}{I_z}
\end{cases}
\tag{7}
$$

where M is the vehicle mass, C_r is the cornering rear stiffness coefficient, l_r is the chassis length rear and I_z is moment of vehicle inertia. The nonlinear dynamic of EPS (4) has three nonlinear sign functions, which are related to coulomb friction [25]. Assume that $T_d = 0$, therefore, the EPS system (4) together with the dynamic (7) can be reformulated in the following state space representation:

$$
\dot x = Ax + Bu + Ensf(x)
\tag{8}
$$

where $x = [\theta_c \quad w_c \quad \theta_m \quad w_m \quad x_r \quad v_r \quad \beta \quad \gamma]^T$ is the state vector, $u = I_m$ is the control input, $nsf(x) = [\mathrm{sgn}(w_c) \quad \mathrm{sgn}(w_m) \quad \mathrm{sgn}(v_r)]^T$ is the signum function vector and

$$
A = \begin{bmatrix}
0 & 1 & 0 & 0 & 0 & 0 & 0 & 0 \\
a_{21} & a_{22} & 0 & 0 & a_{25} & 0 & 0 & 0 \\
0 & 0 & 0 & 1 & 0 & 0 & 0 & 0 \\
0 & 0 & a_{43} & a_{44} & a_{45} & 0 & 0 & 0 \\
0 & 0 & 0 & 0 & 0 & 1 & 0 & 0 \\
a_{61} & 0 & a_{63} & 0 & a_{65} & a_{66} & a_{67} & a_{68} \\
a_{71} & 0 & 0 & 0 & 0 & 0 & a_{77} & a_{78} \\
a_{81} & 0 & 0 & 0 & 0 & 0 & a_{87} & a_{88}
\end{bmatrix}
$$

$$
a_{21} = -\frac{K_c}{j_c}; \quad a_{22} = -\frac{B_c}{j_c}; \quad a_{25} = \frac{K_c}{j_c r_p}; \quad a_{43} = -\frac{K_m}{j_m}
$$

$$
a_{44} = -\frac{B_m}{j_m}; \quad a_{45} = \frac{K_m G_G}{j_m r_p}; \quad a_{61} = \frac{K_c G_{sc} - T_p C_f}{M_r r_p G_{sc}}
$$

$$
a_{63} = \frac{G_G k_m}{M_r r_p}; \quad a_{65} = -\frac{K_t r_p^2 + K_c + G_G^2 K_m}{M_r r_p^2}; \quad a_{66} = -\frac{B_r}{M_r}
$$

$$
a_{67} = \frac{T_p C_f}{M_r r_p}; \quad a_{68} = \frac{I_f T_p C_f}{M_r r_p V}; \quad a_{71} = \frac{C_f}{MVG_{sc}}
$$

$$
a_{77} = -\frac{C_f + C_r}{MV}; \quad a_{78} = \frac{l_f C_f - l_r C_r - MV^2}{MV^2}; \quad a_{81} = \frac{l_f C_f}{I_z G_{sc}}
$$

$$
a_{87} = \frac{l_r C_r - l_f C_f}{I_z}; \quad a_{88} = -\frac{l_f^2 C_f + l_r^2 C_r}{VI_z}
$$

$$
B = \begin{bmatrix} 0 & 0 & 0 & \frac{K_a}{j_m} & 0 & 0 & 0 & 0 \end{bmatrix}^T
$$

$$
E = \begin{bmatrix}
0 & -\frac{F_c}{j_c} & 0 & 0 & 0 & 0 & 0 & 0 \\
0 & 0 & 0 & -\frac{F_m}{j_m} & 0 & 0 & 0 & 0 \\
0 & 0 & 0 & 0 & 0 & -\frac{F_r}{M_r} & 0 & 0
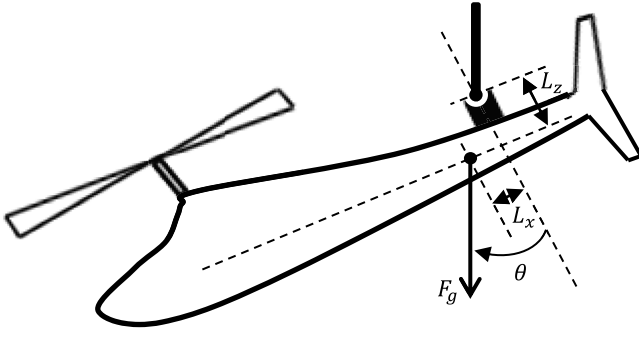\end{bmatrix}^T.
$$

This article has been accepted for inclusion in a future issue of this journal. Content is final as presented, with the exception of pagination.

4

IEEE TRANSACTIONS ON SYSTEMS, MAN, AND CYBERNETICS: SYSTEMS

Fig. 2. Diagram of the helicopter system.

Fig. 3. Diagram of the servo-system with backlash and Coulomb friction.

B. Helicopter System

Another practical example, whose dynamics can be formulated as in (1), is a rotorcraft system. A state space model was built for an experimental setup of a two-degrees-of-freedom helicopter in [20]. Consider a simplified version of the nonlinear pitch model of the helicopter as follows [11]:

$$
\begin{cases}
\dot{\theta} = w \\
\dot{w} = \frac{1}{I_{yy}}\left(\begin{array}{l} -mL_xg\cos(\theta) - mL_zg\sin(\theta) \\ -F_{km}\mathrm{sgn}(w) - F_{vm}w + u \end{array} \right)
\end{cases} \tag{9}
$$

where θ and w denote the pitch angle and pitch rate of the helicopter and the definitions of the system parameters are given in [11]. The schematic of the helicopter system is drawn in Fig. 2.

The equilibrium point is $x_1 = -\arctan(L_x/L_z)$ and $x_2 = 0$. The goal is to stabilize the system (9) at the origin [11]. Therefore, an offset input is needed. The dynamic equations (9) can be transformed in such way that the equilibrium point will be at the origin

$$
\begin{cases}
\dot{x}_1 = x_2 \\
\dot{x}_2 = \frac{1}{I_{yy}}\left(\begin{array}{l} mL_xg - mL_xg\cos(x_1) \\ -mL_zg\sin(x_1) - F_{km}\mathrm{sgn}(x_2) - F_{vm}x_2 \\ + u - mL_xg \end{array} \right)
\end{cases} \tag{10}
$$

where $x = [x_1 \ x_2]^T = [\theta \ w]^T$ is the state vector. In the following, we are interested in deriving the equivalent TS model of (10). There exist two nonlinear terms $z_1 = mL_xg - mL_xg\cos(x_1) - mL_zg\sin(x_1)$ and $z_2 = \mathrm{sgn}(x_2)$. The term z_1 satisfies the sector nonlinearity condition [18]

$$
a_1x_1 \leq z_1 \leq a_2x_2 \tag{11}
$$

with $a_1 = -0.3034$ and $a_2 = 0.1076$. Based on the (11), one has

$$
\begin{cases}
z_1 = h_1(x_1)a_1x_1 + h_2(x_1)a_2x_1 \\
h_1(x_1) = \frac{a_2x_1 - z_1}{(a_2-a_1)x_1}; \ h_2(x_1) = \frac{z_1 - a_1x_1}{(a_2-a_1)x_1}.
\end{cases} \tag{12}
$$

The term z_2 comprises the signum function that cannot be exactly represented by a TS model. Substituting (12) into (10) provides an equivalent two-rule TS model as

$$
\dot{x} = \sum_{i=1}^{2} h_i(x)\left(A_ix + B_iu^* + E_insf(x)\right) \tag{13}
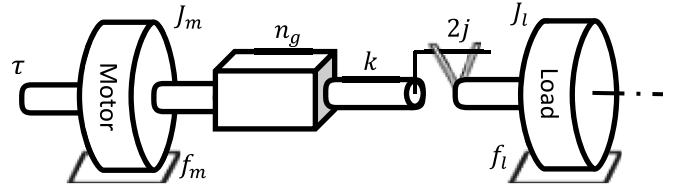$$

where the normalized membership functions are defined by (12), $u^* = u - mL_xg$ is the new control input, $nsf(x) = -\mathrm{sgn}(x_2)$ is the sign function vector and

$$
A_1 = \begin{bmatrix} 0 & 1 \\ \frac{a_1}{I_{yy}} & -\frac{F_{vm}}{I_{yy}} \end{bmatrix}; \ A_2 = \begin{bmatrix} 0 & 1 \\ \frac{a_2}{I_{yy}} & -\frac{F_{vm}}{I_{yy}} \end{bmatrix}
$$

$$
B_1 = B_2 = \begin{bmatrix} 0 \\ 1/I_{yy} \end{bmatrix}; \ E_1 = E_2 = \begin{bmatrix} 0 \\ F_{km}/I_{yy} \end{bmatrix}.
$$

C. Servo-System

Consider the dynamics of the servo-system with flexible shaft [10]

$$
J_m\ddot{\theta}_m + c_m\dot{\theta}_m + f_m\mathrm{sgn}(\dot{\theta}_m) + T(\Delta_\theta) = \tau
$$
$$
J_l\ddot{\theta}_l + c_l\dot{\theta}_l + f_l\mathrm{sgn}(\dot{\theta}_l) = nT(\Delta_\theta) \tag{14}
$$

where θ_m and θ_l are the angular position of the motor and the load, and τ is the input torque. In addition, J_m and J_l are the inertia of the motor and the load, f_m and f_l are the dry friction of the motor and the load, c_m and c_l are the viscous friction of the motor and the load, and n_g is the gear reduction ratio. Furthermore, $T(\Delta_\theta)$ represents the transmitted torque from the motor to the load. The $T(\Delta_\theta)$ is formulated by the following dead zone model:

$$
T(\Delta_\theta) = \begin{cases} 0, & \text{if } |\Delta_\theta| \leq j \\ kn_q^{-2}(\Delta_\theta - j\mathrm{sgn}(\Delta_\theta)), & \text{otherwise} \end{cases} \tag{15}
$$

where $\Delta_\theta = \theta_m - n_g\theta_l$, k is the torsional spring stiffness and j is the backlash amplitude. The diagram of the servo-system is presented in Fig. 3.

Equation (15) is equivalent to

$$
T(\Delta_\theta) = T_1(\Delta_\theta) + T_2(\Delta_\theta) \tag{16}
$$

where $T_1(\Delta_\theta) = kn_g^{-2}\Delta_\theta$ is the linear term and $T_2(\Delta_\theta)$ is the nonsmooth saturation term

$$
T_2(\Delta_\theta) = \begin{cases} -kn_g^{-2}\Delta_\theta, & \text{if } |\Delta_\theta| \leq j \\ -kn_g^{-2}j\mathrm{sgn}(\Delta_\theta), & \text{otherwise.} \end{cases} \tag{17}
$$

The overall dead zone characteristics $T(\Delta_\theta)$ and the linear and nonlinear parts $T_1(\Delta_\theta)$ and $T_2(\Delta_\theta)$, are drawn in Fig. 4. As it can be seen in Fig. 4, the saturation function $T_2(\Delta_\theta)$ is bounded.

By substituting (16) and (17) into (14) and applying some simplifications, the following sate space representation of the

This article has been accepted for inclusion in a future issue of this journal. Content is final as presented, with the exception of pagination.

VAFAMAND *et al.*: TS FUZZY MODEL-BASED CONTROLLER DESIGN FOR CLASS OF NONLINEAR SYSTEMS
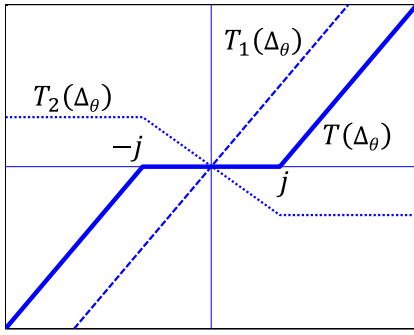
5

Fig. 4.   Nonsmooth dead zone model.

servo-system will be achieved:

$$
\begin{bmatrix} \dot{x}_1 \\ \dot{x}_2 \\ \dot{x}_3 \\ \dot{x}_4 \end{bmatrix} = \begin{bmatrix} 0 & 1 & 0 & 0 \\ -J_m^{-1}kn_g^{-2} & -J_m^{-1}c_m & J_m^{-1}kn_g^{-1} & 0 \\ 0 & 0 & 0 & 1 \\ J_l^{-1}kn_g^{-1} & 0 & -J_l^{-1}k & -J_l^{-1}c_l \end{bmatrix}
$$
$$
\times \begin{bmatrix} x_1 \\ x_2 \\ x_3 \\ x_4 \end{bmatrix} + \begin{bmatrix} 0 \\ J_m^{-1} \\ 0 \\ 0 \end{bmatrix} u + \begin{bmatrix} 0 & 0 \\ 1 & 0 \\ 0 & 0 \\ 0 & 1 \end{bmatrix} nsf(x). \quad (18)
$$

where $x = [x_1 \ x_2 \ x_3 \ x_4]^T = [\theta_m \ \dot{\theta}_m \ \theta_l \ \dot{\theta}_l]^T$ is the state vector, $u = \tau$ is the control input and $nsf(x) = [\ -J_m^{-1}f_m\mathrm{sgn}(x_2) - J_m^{-1}T_2(\Delta_\theta) - J_l^{-1}f_l\mathrm{sgn}(x_4) + J_l^{-1}T_2(\Delta_\theta)]^T$ is the nonsmooth function vector. Equivalently, by defining a new control input

$$
u' = u - f_m\mathrm{sgn}(x_2) - T_2(\Delta_\theta) \quad (19)
$$

and substituting into (18), one has

$$
\begin{bmatrix} \dot{x}_1 \\ \dot{x}_2 \\ \dot{x}_3 \\ \dot{x}_4 \end{bmatrix} = \begin{bmatrix} 0 & 1 & 0 & 0 \\ -J_m^{-1}kn_g^{-2} & -J_m^{-1}c_m & J_m^{-1}kn_g^{-1} & 0 \\ 0 & 0 & 0 & 1 \\ J_l^{-1}kn_g^{-1} & 0 & -J_l^{-1}k & -J_l^{-1}c_l \end{bmatrix}
$$
$$
\times \begin{bmatrix} x_1 \\ x_2 \\ x_3 \\ x_4 \end{bmatrix} + \begin{bmatrix} 0 \\ J_m^{-1} \\ 0 \\ 0 \end{bmatrix} u' + \begin{bmatrix} 0 \\ 0 \\ 0 \\ 1 \end{bmatrix} nsf'(x) \quad (20)
$$

where $nsf'(x) = -J_l^{-1}f_l\mathrm{sgn}(x_4) + J_l^{-1}T_2(\Delta_\theta)$. The dynamic equations (18) and (20) are in the form (2).

In the following, we will discuss our TS-based fuzzy approach in tackling with the class of nonsmooth state space representation (2).

III. NEW APPROACH FOR HANDLING SIGNUM FUNCTIONS

In this section, first, BIBO stability analysis and L_1 performance criterion will be defined. Then, nonquadratic Lyapunov function (NQLF) and non-PDC controller will be presented. Finally, the main results of this paper will be proposed.

A. Nonsmooth Function As Persistent Bounded Disturbance

As discussed before, the nonsmooth functions cannot be exactly represented by a TS fuzzy model [19], [21], [22]. In this paper, a novel method is proposed for TS fuzzy handling nonsmooth terms in the model. In this approach, the nonsmooth functions are considered as a disturbance vector. The main property of the signum and saturation functions is the inherit boundedness that characterizes the disturbance as a persistent bounded signal. The persistent bounded disturbance belongs to L_∞ space and generally does not converge to zero when $t \to \infty$ [31]. It should be noted that, considering signum function as disturbance, does not change the behavior of the original system and the system equilibrium point is maintained at the origin. This is achieved by the fact that $nsf(0) = 0$.

By defining the persistent bounded disturbance, the goal is to design a robust controller such that the effect of the disturbance on the closed-loop system output is minimized. For this type of disturbances, one can guarantee the boundedness of the system state vector as $t \to \infty$. Therefore, the stabilization conditions are derived through bounded input-bounded output (BIBO) stability criterion and the robust controller design conditions are obtained based on L_1 performance index.

B. L_1 Performance Criterion

The optimal L_1 performance problem is to design a robust controller, such that the following problem is guaranteed for the closed-loop TS system:

$$
\min_u \sup_{x \neq 0} \frac{\|y\|_\infty}{\|nsf(x)\|_\infty} = \min_u \sqrt{\sup_{x \neq 0} \frac{y^T y}{nsf(x)^T nsf(x)}}
$$
$$
\leq \Omega \quad (21)
$$

where the infinity norm of a vector signal is defined as [32]

$$
\|v\|_\infty^2 = \sup_{t \geq 0} v(t)^T v(t). \quad (22)
$$

In the definition (21), the ratio of the infinity norm of the output with respect to the infinity norm of the disturbance is considered which is different from those presented in [31] and [33]. In [31] and [33], the ratio of the infinity norm of the state with respect to the infinity norm of the disturbance is utilized. Therefore, the peak of the output vector y can be reduced by the level Ω under the effect of the peak of the persistent bounded disturbance $nsf(x)$. The L_1 performance (21) is modified as

$$
\|y\|_\infty < \Phi|y(0)| + \Omega\|nsf(x)\|_\infty \quad (23)
$$

where Φ is a positive scalar.

C. Slack Matrices and Fruitful Lemmas

In this section, we will present some fruitful slack matrices and lemmas that will be used in the proof procedure of the main results. Based on the convex sum property of membership functions (3), the following null term is defined [34]:

$$
\sum_{\rho=1}^r \dot{h}_\rho \begin{bmatrix} \sum_{i=1}^r \frac{P_i}{r} - \frac{M}{r} & 0 \\ 0 & 0 \end{bmatrix} = 0 \quad (24)
$$

This article has been accepted for inclusion in a future issue of this journal. Content is final as presented, with the exception of pagination.

6   IEEE TRANSACTIONS ON SYSTEMS, MAN, AND CYBERNETICS: SYSTEMS

where M is a symmetric matrix with appropriate dimensions. The null term (24) will be added to the time derivative of NQLF to obtain more relaxed conditions.

Lemma 1 [31]: If a real scalar function $S(t)$ satisfies the differential inequality

$$\dot{S}(t) \leq -\alpha S(t) + \beta v(t) \tag{25}$$

where α and β are positive scalar, then

$$S(t) \leq e^{-\alpha t} S(0) + \beta \int_0^t e^{-\alpha \tau} v(t-\tau) d\tau. \tag{26}$$

Lemma 2 [35]: Inequality $\sum_{i=1}^r \sum_{j=1}^r h_i h_j \gamma_{ij} < 0$ is satisfied if

$$\begin{cases} \gamma_{ii} < 0, \\ \frac{2}{r-1} \gamma_{ii} + \gamma_{ij} + \gamma_{ji} < 0, \end{cases} \quad \text{for } i \neq j < 1, \ldots, r. \tag{27}$$

Lemma 3 [18]: The nonperturbed open-loop TS system (2) (i.e., $E_i = 0$) is asymptotically stabilizable with PDC controller $u = \sum_{i=1}^r h_i(z(t)) K_i x(t)$ with the decay rate α, if there exists matrices $X = X^T > 0$ and S_i such that

$$\begin{cases} XA_i^T + A_i X + S_i^T B_i^T + B_i S_i + \alpha X & < 0 \\ \begin{pmatrix} X(A_i^T + A_j^T) + (A_i + A_j)X + S_j^T B_i^T \\ + B_j S_i + S_j^T B_i^T + B_i S_j + 2\alpha X \end{pmatrix} & < 0. \end{cases} \tag{28}$$

Furthermore, the controller gains are obtained as $K_i = S_i X^{-1}$.

Lemmas 1 and 2 will be used in the main results of this paper in Section IV. In addition, Lemma 3 will be used in Section V.

IV. MAIN RESULTS

In this section, first, the NQLF and non-PDC controller are presented. Then, through the BIBO stability, the sufficient conditions that assure the boundedness of the closed-loop TS systems including bounded nonsmooth functions are derived.

A. Lyapunov Function and State Feedback Controller

To obtain BIBO conditions, the NQLF and the non-PDC controller are considered as follows:

$$V(x(t)) = x(t)^T P_z^{-1} x(t) \tag{29}$$

$$u(t) = \sum_{i=1}^r h_i(z(t)) F_i P_z^{-1} x(t) \tag{30}$$

where $P_z = \sum_{\rho=1}^r h_\rho(z(t)) P_\rho$ with $P_i = P_i^T > 0$ and F_i are the local feedback gains with appropriate dimensions. By substituting the non-PDC (30) into the open-loop TS system (2), closed-loop system will be obtained as

$$\dot{x}(t) = \sum_{i=1}^r \sum_{j=1}^r h_i(z(t)) h_j(z(t)) \{A_i P_j + B_i F_j\} P_z^{-1} x(t)$$

$$+ \sum_{i=1}^r h_i(z(t)) E_i nsf(t). \tag{31}$$

In the following, sufficient conditions will be derived in terms of LMIs such that the closed-loop TS system (31) guarantees the L_1 performance criterion (21).

B. Controller Design Conditions

The next theorem provides sufficient conditions to minimize the peak-to-peak level performance of the closed-loop TS system.

Theorem 1: Suppose that the time derivatives of the membership functions in the closed-loop system (31) have known lower bounds $-\varphi_\rho$ such that

$$-\varphi \leq -\varphi_\rho \leq \dot{h}_\rho \tag{32}$$

For a given positive scalar α, if there exist symmetric matrices M and P_i and matrices F_i for $i = 1, \ldots, r$ such that the following LMIs are satisfied:

$$P_i > 0 \quad \text{for } i \leq r \tag{33}$$

$$P_\rho - \sum_{i=1}^r \frac{P_i}{r} + \frac{M}{r} > 0, \quad \text{for } \rho \leq r \tag{34}$$

$$\begin{cases} Q_{ii} < 0, & \text{for } i \leq r \\ \frac{2}{r-1} Q_{ii} + Q_{ij} + Q_{ji} < 0, & \text{for } i < j \leq r \end{cases} \tag{35}$$

$$\begin{cases} W_{ii} > 0, & \text{for } i \leq r \\ \frac{2}{r-1} W_{ii} + W_{ij} + W_{ji} > 0, & \text{for } i < j \leq r \end{cases} \tag{36}$$

where

$$Q_{ij} = \begin{bmatrix} \text{sym}(A_i P_j + B_i F_j) + \alpha P_j + \varphi M & E_i \\ E_i^T & -\beta I \end{bmatrix}$$

$$W_{ij} = \begin{bmatrix} \alpha P_i & 0 & P_i C_j^T \\ 0 & (\gamma - \beta)I & 0 \\ C_j P_i & 0 & \gamma I \end{bmatrix}.$$

Then, the peak to peak (L_1) performance in (23) is guaranteed with an attenuated level $\Omega = \gamma$. Moreover, and the local feedback matrices of non-PDC controller (30) are derived.

Proof: Substituting the closed-loop system (31) into the time derivative of NQLF (29) yields

$$\dot{V}_Q = \begin{bmatrix} P_z^{-1} x \\ nsf(x) \end{bmatrix}^T \begin{bmatrix} \text{sym}(A_z P_z + B_z F_z) - \dot{P}_z & E_z \\ E_z^T & 0 \end{bmatrix} \begin{bmatrix} P_z^{-1} x \\ nsf(x) \end{bmatrix} \tag{37}$$

where $\text{sym}(H) = H + H^T$. Adding and subtracting the term $\alpha x^T P_z^{-1} P_z P_z^{-1} x + \beta nsf(x)^T nsf(x)$ with positive scalars α and β results in

$$\dot{V}_Q = \begin{bmatrix} P_z^{-1} x \\ nsf(x) \end{bmatrix}^T \begin{bmatrix} \begin{pmatrix} \text{sym}(A_z P_z + B_z F_z) \\ -\dot{P}_z + \alpha P_z \end{pmatrix} & E_z \\ E_z^T & -\beta I \end{bmatrix} \begin{bmatrix} P_z^{-1} x \\ nsf(x) \end{bmatrix}$$

$$- \alpha x^T P_z^{-1} x + \beta nsf(x)^T nsf(x). \tag{38}$$

By defining Γ_1 as

$$\Gamma_1 = \begin{bmatrix} \text{sym}(A_z P_z + B_z F_z) - \dot{P}_z + \alpha P_z & E_z \\ E_z^T & -\beta I \end{bmatrix} \tag{39}$$

where I is the identity matrix of appropriate dimensions. In the following, sufficient conditions will be proposed in terms of LMIs to guarantee the negative definiteness of Γ_1. By adding the null term (24) to (39), Γ_1 will be continued as

$$\Gamma_1 = \sum_{i=1}^r \sum_{j=1}^r \begin{bmatrix} \begin{pmatrix} \text{sym}(A_i P_j + B_i F_j) + \alpha P_j \\ -\sum_{\rho=1}^r \dot{h}_\rho (P_\rho - \sum_{i=1}^r \frac{P_i}{r} + \frac{M}{r}) \end{pmatrix} & E_i \\ E_i^T & -\beta I \end{bmatrix}. \tag{40}$$

This article has been accepted for inclusion in a future issue of this journal. Content is final as presented, with the exception of pagination.

VAFAMAND *et al.*: TS FUZZY MODEL-BASED CONTROLLER DESIGN FOR CLASS OF NONLINEAR SYSTEMS

7

Using (32) and (34), one concludes that

$$-\sum_{\rho=1}^{r} \dot{h}_\rho \left(P_\rho - \sum_{i=1}^{r} \frac{P_i}{r} + \frac{M}{r} \right) < \varphi M. \tag{41}$$

Therefore, $\Gamma_1 \leq \Gamma_2$, where Γ_2 equals to

$$\Gamma_2 = \sum_{i=1}^{r} \sum_{j=1}^{r} \begin{bmatrix} \left\{ \begin{matrix} \text{sym}(A_i P_j + B_i F_j) \\ +\alpha P_j + \varphi M \end{matrix} \right\} & E_i \\ E_i^T & -\beta I \end{bmatrix}. \tag{42}$$

Based on Lemma 3, the negative definiteness of (42) is enforced if the LMIs (35) are satisfied. Therefore, from (38), one has

$$\dot{V}_Q \leq -\alpha x^T P_z^{-1} x + \beta nsf(x)^T nsf(x)$$
$$= -\alpha V_Q + \beta nsf(x)^T nsf(x). \tag{43}$$

Considering Lemma 1, we obtain

$$x^T P_z^{-1} x \leq e^{-\alpha t} x(0)^T P_{z0}^{-1} x(0) + \beta \int_0^t e^{-\alpha\tau} nsf(x(t-\tau))^T nsf$$
$$\times (x(t-\tau)) d\tau$$
$$\leq \sup_{\tau \in [0,t]} \left\{ e^{-\alpha t} x(0)^T P_{z0}^{-1} x(0) + \beta \int_0^t e^{-\alpha\tau} nsf(x(t-\tau))^T \right.$$
$$\left. \times nsf(x(t-\tau)) d\tau \right\}$$
$$\leq x(0)^T P_{z0}^{-1} x(0) + \frac{\beta}{\alpha} \|nsf(x)\|^T \|nsf(x)\| \tag{44}$$

where $P_{z0} = \sum_{i=1}^{r} h_i(z(0)) P_i$. Utilizing (2), one can write the following equality for the system output:

$$y^T y = \begin{bmatrix} x^T & nsf(x)^T \end{bmatrix} \begin{bmatrix} C_z^T \\ 0 \end{bmatrix} \begin{bmatrix} C_z & 0 \end{bmatrix} \begin{bmatrix} x \\ nsf(x) \end{bmatrix}. \tag{45}$$

Now, suppose that the following inequality holds:

$$y^T y \leq \gamma \begin{bmatrix} x^T P_z^{-1} & nsf(x)^T \end{bmatrix} \begin{bmatrix} \alpha P_z & 0 \\ 0 & (\gamma-\beta)I \end{bmatrix} \begin{bmatrix} P_z^{-1} x \\ nsf(x) \end{bmatrix}. \tag{46}$$

Then, we have

$$y^T y \leq \gamma \left(\alpha x^T P_z^{-1} x + (\gamma-\beta) nsf(x)^T nsf(x) \right). \tag{47}$$

Substituting (44), results in

$$y^T y \leq x(0)^T P_{z0}^{-1} x(0) + \gamma^2 nsf(x)^T nsf(x). \tag{48}$$

Therefore, the L_1 performance will be

$$\Omega = \sup_{x \neq 0} \frac{\|y\|_\infty}{\|nsf(x)\|_\infty} = \sqrt{\sup_{x \neq 0} \frac{y^T y}{nsf(x)^T nsf(x)}} = \gamma. \tag{49}$$

The remaining issue is to derive sufficient conditions for satisfying (46). By applying Schur complement and Lemma 2, (46) is implied by the LMIs (35). The proof is completed. ∎

Remark 1: In Theorem 1, the sufficient conditions of robust controller design is derived such that the effect of nonsmooth functions on the system output is minimized. However, by decreasing this effect, a higher amplitude control input is achieved. In practice, we encounter physical restrictions on employing amplitude-bounded inputs. Therefore, instead of minimizing the L_1 performance gain in Theorem 1, we may choose this gain in prior. It should be noted that although our

approach assures the BIBO stability with a threshold value of γ, in most cases, the ultimate bound of the system outputs affected by the disturbance are very less than the prechosen parameter. This property can be observed in the simulation section.

Remark 2: In comparison with the existing methods based on the NQLF and the non-PDC scheme [18]–[23], the proposed control method considers the BIBO stability analysis. Deriving the LMI formulations based on the BIBO scheme has some difficulties over the conventional Lyapunov stability theory: 1) negative definiteness of matrices cannot be directly assured due to the existence of zero diagonal elements and 2) establishing a proper relation between the system output and the nonsmooth functions through the BIBO scheme. These difficulties are addressed in this paper, by introducing the null terms in (38) and applying the norm inequalities in (44) and (48).

Remark 3: In several practical systems, the source of the nonlinearity is the signum function appearing in the dynamic equation of the system [10], [24], [28], [36], [37]. Therefore, by considering the nonsmooth signum functions as persistent bounded disturbance, a linear system will be remained. Consequently, the nonlinear TS fuzzy (2) alters to a linear system

$$\dot{x} = Ax + Bu + Ensf(x)$$
$$y = Cx. \tag{50}$$

Furthermore, the nonlinear non-PDC controller (30) turns to a linear one

$$u = FP^{-1}x \tag{51}$$

where $P = P^T > 0$ is the common Lyapunov matrix and F is the controller feedback gains. For this special case, we will present following corollary.

Corollary 1: For the system (50) and controller (51), the peak to peak (L_1) performance in (23) is guaranteed with an attenuated level $\Omega = \gamma$, if there exist symmetric matrix P and matrix F such that the following LMIs are satisfied:

$$P > 0 \tag{52}$$

$$Q = \begin{bmatrix} \text{sym}(AP+BF)+\alpha P & E \\ E^T & -\beta I \end{bmatrix} < 0 \tag{53}$$

$$W = \begin{bmatrix} \alpha P & 0 & PC^T \\ 0 & (\gamma-\beta)I & 0 \\ CP & 0 & \gamma I \end{bmatrix} > 0. \tag{54}$$

Proof: Let $A_i = A$, $B_i = B$, $C_i = C$, $E_i = E$, and $P_i = P$ for $i \leq r$ and $M = 0$ in the conditions of Theorem 1. Consequently, the conditions of Corollary 1 are obtained. The proof is completed. ∎

Remark 4: Fig. 5 illustrates the general schematic of the proposed robust controller design procedure for nonlinear systems with nonsmooth function.

V. SIMULATION

In this section, to show the advantages of the proposed approach in controlling the nonlinear dynamic systems including signum functions, we consider the EPS, helicopter, and
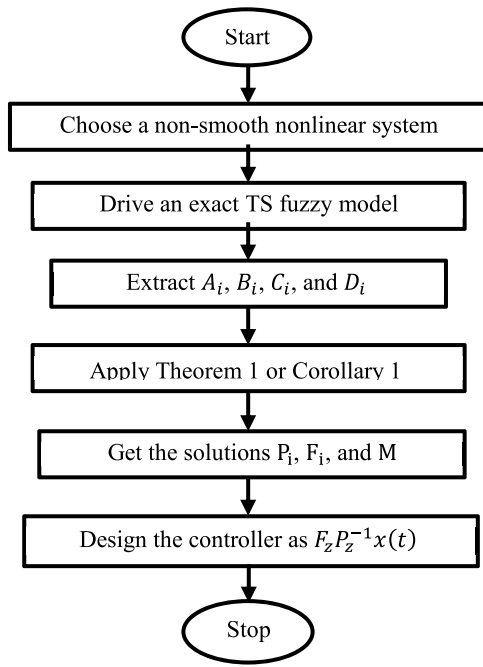
Fig. 5.   Design procedure of the proposed controller.

Fig. 6.   Real time experimental setup.

servo-systems presented in Sections II-A–II-C, respectively. Corollary 1 and Theorem 1 will be applied to these systems and the results will be compared with two recently published works that approximate signum functions by TS fuzzy models [24] and polynomial functions [11], respectively.

In order to evaluate the performance of the proposed control method, the hardware-in-the loop (HIL) simulation approach is utilized. The real time HIL method is used to emulate errors and delays that do not exist in the classical offline simulations. The HIL setup is illustrated in Fig. 6 and is consisting of: 1) OPAL-RT as a real time simulator; 2) a PC as the command station (programming host) in which the MATLAB/Simulink-based code executed on the OPAL-RT is generated; and 3) a router used as a connector of all the setup devices in the same subnetwork. The OPAL-RT is also connected to the DK60 board through Ethernet port.

A. EPS System

Consider the nonlinear dynamic equation (8) with the parameters given in Table I.

By considering the nonlinear signum functions as persistent bounded disturbance, the dynamic equation (8) turns into a linear system with disturbance. Consequently, a simple linear

TABLE I
VALUES OF EPS MODEL PARAMETERS

Symbol	Value	Symbol	Value
j_c	$11.4\ Kg.m^2$	M_r	$32\ kg$
B_c	$0.072\ N.ms/rad$	F_r	$0.002\ N.m$
K_c	$114.6\ N.m/rad$	l_r	$1.8\ m$
F_c	$0.0052\ N.m$	C_r	$126 \times 10^3\ N/rad$
j_m	$5 \times 10^{-4}\ Kg.m^2$	B_r	$13920\ N.ms/rad$
B_m	$0.032\ N.ms/rad$	l_f	$1\ m$
K_m	$125\ N.m$	C_f	$126 \times 10^3\ N/rad$
F_m	$0.0052\ N.m$	r_p	$0.007\ m$
K_a	$5 \times 10^4\ N.m/A$	T_p	$0.033\ m$
K_t	$32900\ N.m$	V	$20\ m/s$
M	$1814\ kg$	G_{Gs}	20

feedback controller of the following form is obtained:

$$I_m = FP^{-1}x = Sx. \tag{55}$$

By letting values $40, 50,$ and 117.3 for α, respectively, in Corollary 1, feedback controller (55) with different matrix gains will be achieved. Each of these feedback matrices is obtained based on the corresponding value of α and specified by a superscript

$$S^1 = \begin{bmatrix} -0.004 & -0.0002 & 0.0022 & 0 & -5.89 & 0 & 0.0143 & -0.028 \end{bmatrix}$$

$$S^2 = \begin{bmatrix} -0.011 & -0.0003 & 0.0021 & 0 & -5.89 & 0 & 0.2064 & -0.131 \end{bmatrix}$$

$$S^3 = \begin{bmatrix} -1.191 & -0.0147 & 0.0031 & 0 & -5.95 & 0 & 319.4 & -70.001 \end{bmatrix}.$$

Furthermore, based on the procedure presented in [24] and [25], the following approximated 2-rule TS model of (8) is achieved:

$$\dot{x} = \sum_{i=1}^{2} h_i(x)(A_i x + B_i u) \tag{56}$$

where the matrices $B_1 = B_2$ are equal to B in (8). Also, the most arrays of $A_1 = [a_{1ij}]$ and $A_2 = [a_{2ij}]$ are the same as the $A = [a_{ij}]$ presented in (8) (i.e., $a_{1ij} = a_{2ij} = a_{ij}$), except

$$a_{122} = -\frac{B_c + F_c}{j_c}; \quad a_{144} = -\frac{B_m + F_m}{j_m}; \quad a_{166} = -\frac{C_f + C_r}{MV}$$

$$a_{222} = \frac{F_c - B_c}{j_c}; \quad a_{244} = \frac{F_m - B_m}{j_m}; \quad a_{266} = \frac{F_r - B_r}{M_r}.$$

Furthermore, the normalized membership functions are obtained as

$$h_1(x) = \frac{x_2 - x_{2\min}}{x_{2\max} - x_{2\min}}; \quad h_2(x) = \frac{x_{2\max} - x_2}{x_{2\max} - x_{2\min}}.$$

By applying the proposed method in [18] (Lemma 3) on (56) and letting $\alpha = 5$, the following feedback gains are achieved:

$$K_1 \cong K_2 \cong \begin{bmatrix} -0.175 & -0.002 & 0.0015 & 0 \\ & -5.90 & 0 & -0.003 & -0.0004 \end{bmatrix}.$$

Fig. 6(a)–(h) illustrates the closed-loop EPS system derived by Corollary 1 with persistent bounded disturbance (C1+PBD) and the PDC controller [18] with approximated TS model [24] (PDC+App. TS). In Corollary 1, a simple linear controller is designed, meanwhile using the approximated TS model [24] with the controller design [18] provides a nonlinear controller. The control input signal and the error of the closed-loop EPS system output are drawn in Figs. 7(a)–(h) and 8(a) and (b).
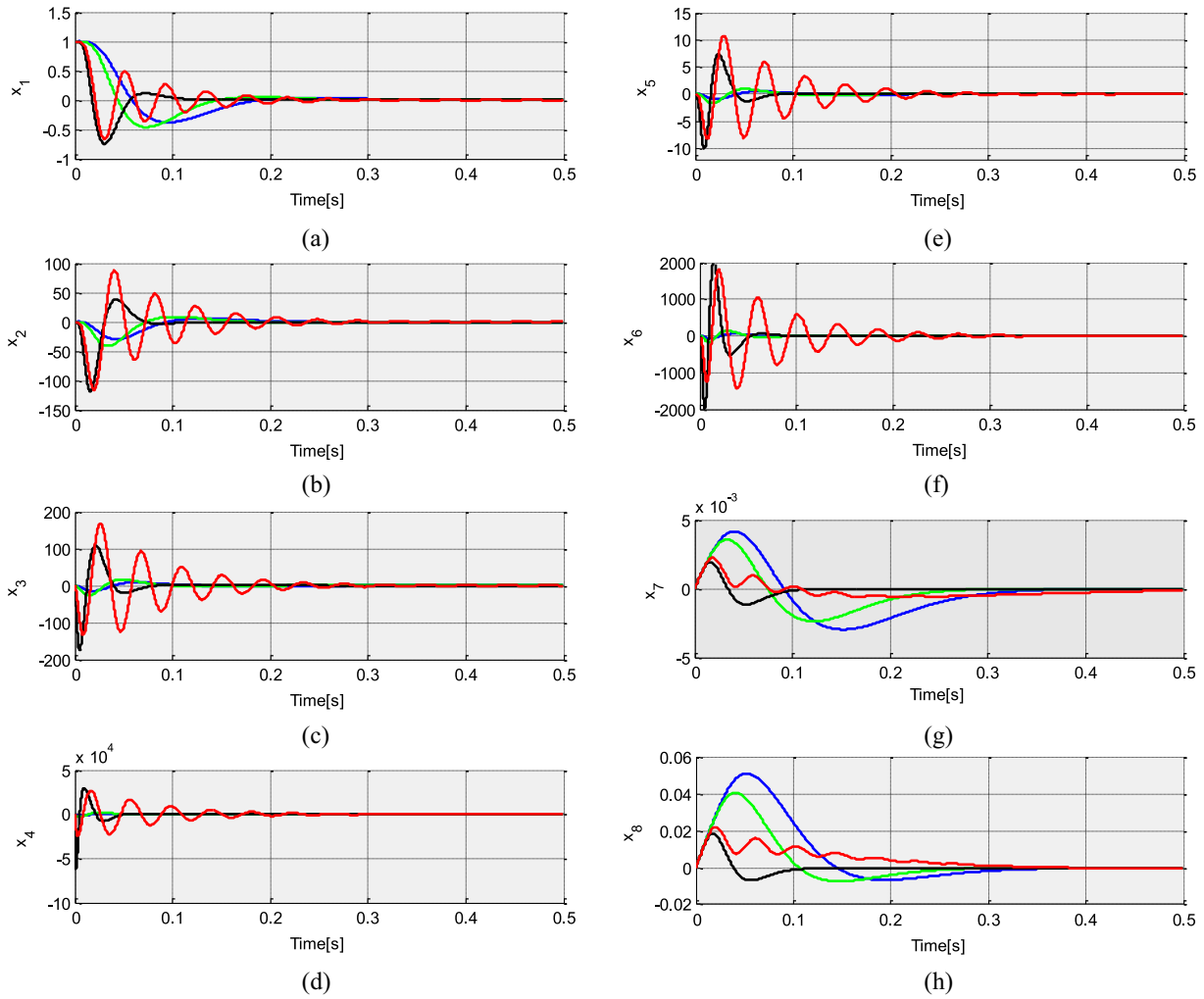
This article has been accepted for inclusion in a future issue of this journal. Content is final as presented, with the exception of pagination.

VAFAMAND *et al.*: TS FUZZY MODEL-BASED CONTROLLER DESIGN FOR CLASS OF NONLINEAR SYSTEMS

9

Fig. 7. EPS state evolutions [C1+PBD ($\alpha = 40$) by "blue," C1+PBD ($\alpha = 50$) by "green," C1+PBD ($\alpha = 117.3$) by "black" and PDC [18]+App. TS [24] by "red"]. (a) State θ_c. (b) State w_c. (c) State θ_m. (d) State w_m. (e) State x_r. (f) State v_r. (g) State β. (h) State γ.

Fig. 7 demonstrates that the four controllers can effectively stabilize the EPS system. However, the first three controllers designed based on the proposed approach in this paper, provide higher steady state performance than the controller design based on the approximated TS system. The reason is that due to the discontinuity of the signum functions, the TS model cannot effectively represent them in the neighborhoods of the origin. Therefore, the behavior of these functions cannot be exactly captured by TS models derived based on linearization method. In some cases (such as the EPS system), the origin is the equilibrium point of system, and the system must be stabilized at origin. Since, the TS model is only an approximation of the original nonlinear including signum function system near the equilibrium point, the controller designed by this TS model does not provide a high performance near the equilibrium point. Thus, the closed-loop system evolution has an oscillatory nature near the equilibrium point that is evident in the Fig. 8(b). This disadvantage in modeling signum functions with TS model is eliminated in the proposed approach of this paper. The robust L_1 controller deign based on the TS modeling with persistent bounded disturbance, can force the states to converge to their equilibrium point without any oscillatory behavior, in this paper.
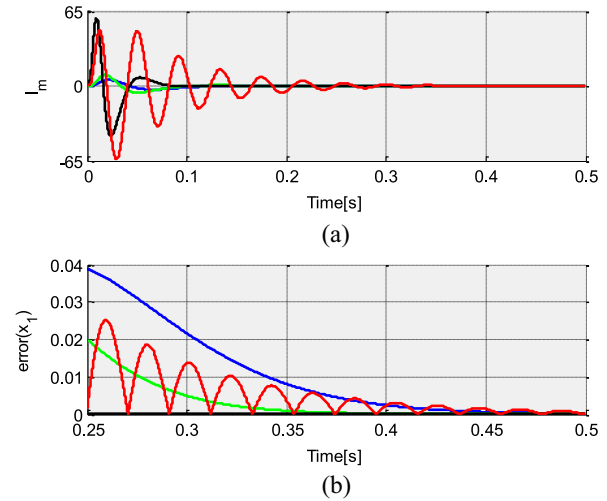

Fig. 8. EPS control input and error of the output, [C1+PBD ($\alpha = 40$) by blue, C1+PBD ($\alpha = 50$) by green, C1+PBD ($\alpha = 117.3$) by black, and PDC [18]+App. TS [24] by red]. (a) Input I_m. (b) Error of the output θ_c.

Furthermore, Table II, demonstrates the L_2 and L_∞ norms of the control input, settling time (0.02%), and L_2 norm of the EPS output.

TABLE II
CONTROL SIGNAL AND OUTPUT EVOLUTION OF EPS SYSTEM

Approach	$\|u\|_\infty$	$\|u\|_2$	Set. Time	$\|error(x_1)\|_2$
C1 ($\alpha = 40$)	5.377	128.490	0.3052	28.7551
C1 ($\alpha = 50$)	9.692	204.808	0.2501	26.5110
C1($\alpha = 117.3$)	59.071	928.746	0.1129	20.4968
App. TS [24]	63.320	1485.34	0.2638	21.9341

TABLE III
VALUES OF HELICOPTER SYSTEM PARAMETERS

Symbol	Value	Symbol	Value
I_{yy}	0.0283 $Kg.m^2$	L_x	0.0134 m
F_{vm}	0.0041 $N.m/s/rad$	L_z	0.0289 m
F_{km}	0.0003 $N.m$	a_1	-0.3034
m	0.9941 Kg	a_2	0.1076

From Table II, one concludes that the fastest transient response is obtained by using $\alpha = 117.3$, has the fastest transient phase. Furthermore, the proposed approach for all values of α provides control laws with less L_∞ and L_2 norms compared to approaches based on the approximated TS models [24]. For instance, by comparing the case C1 ($\alpha = 40$) and [24], it is evident that the energy of the control input of the proposed approach is extensively reduces the energy (more than 11 times smaller than [24]). In addition, in the viewpoint of EPS system output, the proposed controllers for $\alpha = 50$ and 117.3, outperform the controller designed based on approximated TS model [24].

B. Helicopter System

Consider the nonlinear dynamic equation (9) with the parameters given in Table III.

By applying Theorem 1 to the TS fuzzy system (13) and choosing $\varphi = 1$ and $\alpha = 1$, 2, and 3, respectively, different controller matrices gains will be achieved. Similar to Section IV-A, each of these feedback matrices is obtained based on the corresponding value of α and specified by a superscript

$$F_1^1 = \begin{bmatrix} 0.348 & -0.788 \end{bmatrix}; F_2^1 = \begin{bmatrix} -0.289 & -0.011 \end{bmatrix}$$

$$P_1^1 = \begin{bmatrix} 1.568 & -1.837 \\ -1.837 & 6.038 \end{bmatrix}; P_2^1 = \begin{bmatrix} 1.566 & -2.038 \\ -2.038 & 6.038 \end{bmatrix}$$

$$F_1^2 = \begin{bmatrix} 1.028 & -3.169 \end{bmatrix}; F_2^2 = \begin{bmatrix} -0.628 & -0.417 \end{bmatrix}$$

$$P_1^2 = \begin{bmatrix} 3.993 & -6.660 \\ -6.660 & 19.013 \end{bmatrix}; P_2^2 = \begin{bmatrix} 4.030 & -7.062 \\ -7.062 & 20.177 \end{bmatrix}$$

$$F_1^3 = \begin{bmatrix} 1.389 & -8.421 \end{bmatrix}; F_2^3 = \begin{bmatrix} -1.008 & -2.617 \end{bmatrix}$$

$$P_1^3 = \begin{bmatrix} 5.860 & -14.072 \\ -14.072 & 54.229 \end{bmatrix}; P_2^3 = \begin{bmatrix} 5.924 & -14.70 \\ -14.70 & 55.490 \end{bmatrix}.$$

In [11], a piecewise affine (PWA) controller is presented that is applicable for systems with discontinuous vector fields. In that paper, the nonlinearities are approximated by PWA functions in several ranges and a polynomial controller is designed via sum-of-squares technique for each area [11].

Figs. 9(a) and (b) and 10(a) and (b) demonstrate the helicopter states evolution and control input efforts for the proposed approach based on Theorem 1 (T1) and the
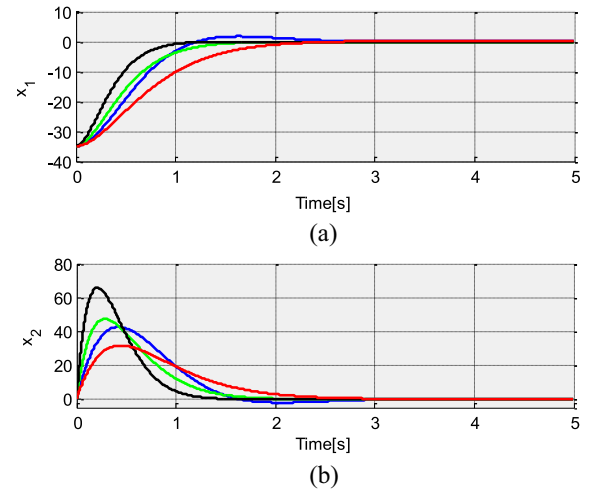

Fig. 9. Helicopter states evolutions, [T1 ($\alpha = 1$) by blue, T1 ($\alpha = 2$) by green, T1 ($\alpha = 3$) by black, and PWA [11] by red]. (a) State θ. (b) State w.
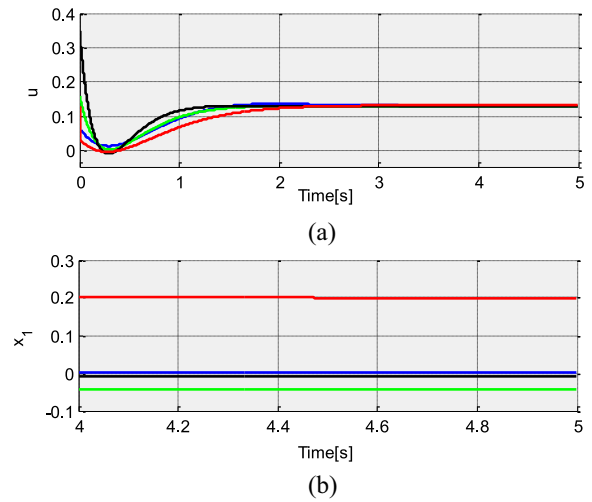

Fig. 10. Helicopter control input and error of the output. (a) u and (b) x_1, (T1 ($\alpha = 1$) by blue, T1 ($\alpha = 2$) by green, T1 ($\alpha = 3$) by black, and PWA [11] by red).

TABLE IV
INPUT AND OUTPUT EVOLUTION OF HELICOPTER SYSTEM

Approach	$\|u\|_\infty$	$\|u\|_2$	Settl. time (0.02%)	Error at t = 4.9 s
T1($\alpha = 1$)	0.1360	8.3576	2.2941	1.8139×10^{-2}
T1($\alpha = 2$)	0.1607	8.3219	1.4757	-4.1712×10^{-2}
T1($\alpha = 3$)	0.3508	8.7527	1.0276	-7.2763×10^{-3}
PWA [11]	0.1320	7.9189	2.1300	0.198

PWA controller in [11]. Both approaches can stabilize the helicopter states and force the pitch angle to converge to its desired reference. However, as it can be seen in Fig. 9(b), the steady state error of the closed-loop system derived based on T1 is close to zero, while the one based on [11] is about 0.2. Therefore, the proposed approach has a better performance compared to [11]. Moreover, it can be seen that by approximate selection of the parameter α in Theorem 1, the steady state error converges sufficiently close to zero.
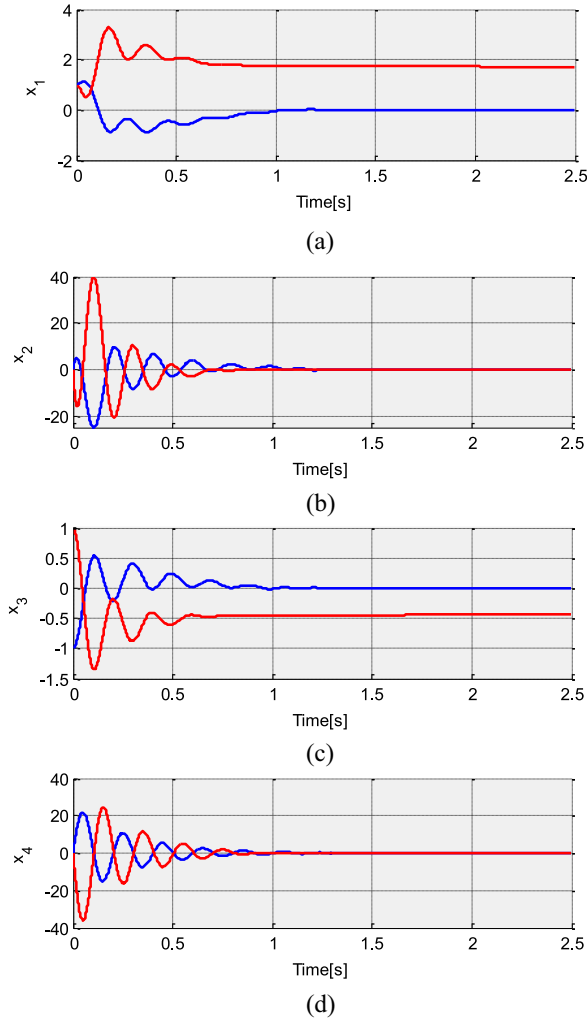
This article has been accepted for inclusion in a future issue of this journal. Content is final as presented, with the exception of pagination.

VAFAMAND *et al.*: TS FUZZY MODEL-BASED CONTROLLER DESIGN FOR CLASS OF NONLINEAR SYSTEMS

11

(a)

(b)

(c)

(d)

Fig. 11.   States (a) x_1, θ_m; (b) x_2, θ_m; (c) x_3, θ_l; and (d) x_4, θ_l (C1 [based on the model (18)] red, C1 [based on the model (20)] by blue).

Table IV demonstrates the metrics of the control input, settling time (0.02%) and the error of the EPS system output at time $t = 4.9$ s.

From Table IV, it is inferred that the proposed approach provides significantly less steady state output error compared to the PWA controller [11]. From the quantitative viewpoint, by comparing the controllers based on the cases T1($\alpha = 1$) and [11], one concludes that the norm-2 and $-\infty$ of the proposed approach is about 1.03 and 1.05 time higher, respectively. However, the steady-state error is reduced about 109 time less than [11]. Consequently, the steady-state performance is greatly improved by the expense of a litter increase in the control input amplitude and energy. Furthermore, by increasing the value of the parameter α, the closed-loop convergence speed of the system and the amplitude and the energy of control effort will be increased.

C. Servo-System

Consider the nonlinear dynamic equation of the servo-system (9) with the parameters given in Table V.

Applying Corollary 1 (C1) with $\alpha = 1$ and $\beta = 5$ to the representations (18) and (20), the following control

TABLE V
VALUES OF SERVO-SYSTEM PARAMETERS

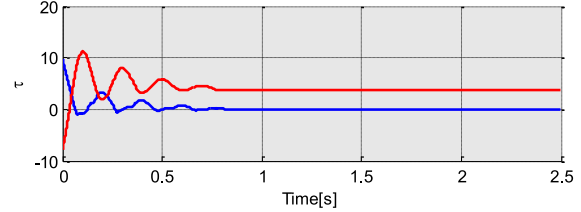| Param.	Value	Param.	Value
J_m	$0.0025\ Kgm^2$	c_m	$0.000394\ N.m.s/rad$
J_l	$0.0271\ Kgm^2$	n_g	4
f_m	$0.036\ N.m$	k	$25.35\ N.m/rad$
f_l	$0.2559\ N.m$	j	$0.7\ rad$
c_l	$0.008\ N.m.s/rad$		

Fig. 12.   Control input: (C1 [based on the model (18)] red, C1 [based on the model (20)] by blue).

signals are provided (each of the feedback matrices is obtained based on the corresponding system matrices and specified by a superscript):

$$u = S^1 x$$
$$S^1 = [0.8001 \quad -0.0676 \quad -9.3101 \quad -0.0733]$$
$$u' = u - f_m\mathrm{sgn}(x_2) + T_2(\Delta_\theta) = S^2 x$$
$$S^2 = [1.1252 \quad -0.0435 \quad -8.0555 \quad -0.0663].$$

Fig. 11 (a)–(d) shows the closed-loop servo-system derived by Corollary 1 based on the (18) and (20). Also, the control input signal and the error of the closed-loop servo-system output are drawn in Fig. 12.

As it can be seen in Fig. 11, the controller designed based on (20) provides a better performance compared to the controller based on (18). In the model (18), the persistent bounded disturbance input is the vector $[-J_m^{-1}f_m\mathrm{sgn}(x_2) - J_m^{-1}T_2(\Delta_\theta) - J_l^{-1}f_l\mathrm{sgn}(x_4) + J_l^{-1}T_2(\Delta_\theta)]$. Meanwhile, in the model (20), a new controller is defined to completely eliminate the effect of the nonsmooth term $-J_m^{-1}f_m\mathrm{sgn}(x_2) - J_m^{-1}T_2(\Delta_\theta)$. Consequently, only the term $-J_l^{-1}f_l\mathrm{sgn}(x_4) + J_l^{-1}T_2(\Delta_\theta)$ is considered as the persistent bounded disturbance input and alleviated by the controller (19). Therefore, the designed controller based on the model (20) improves the closed-loop system performance.

VI. Conclusion

This paper proposes a novel robust controller design for a class of nonlinear systems including hard nonlinearity signum and saturation functions. The proposed approach is based on TS fuzzy modeling, NQLF and non-PDC scheme. By employing the sector nonlinearity approach, this class of systems is represented by TS fuzzy models. The main advantage of this modeling is that no approximation due to existence of the discontinuous hard nonlinearities is accomplished. Therefore, the obtained TS fuzzy model can exactly represent the original nonlinear system. Based on the inherit properties of signum functions, the BIBO stability scheme,

This article has been accepted for inclusion in a future issue of this journal. Content is final as presented, with the exception of pagination.

12   IEEE TRANSACTIONS ON SYSTEMS, MAN, AND CYBERNETICS: SYSTEMS

and L_1 performance criterion are considered. Consequently, new robust controller design conditions are derived in terms of LMIs. EPS system, helicopter model, and servo-system are studied as three case studies. In these systems, the friction forces are modeled by signum functions. Experimental simulation results illustrate that the proposed controller can force the states to converge to their equilibrium point without any oscillation behavior. For the future work, deriving the local stability analysis for the class of nonlinear systems with nonsmooth function can be a good research area.

REFERENCES

[1] R. I. Leine and H. Nijmeijer, *Dynamics and Bifurcations of Non-Smooth Mechanical Systems*, vol. 18. Heidelberg, Germany: Springer, 2013.

[2] Y. Jin, P. H. Chang, M. Jin, and D. G. Gweon, "Stability guaranteed time-delay control of manipulators using nonlinear damping and terminal sliding mode," *IEEE Trans. Ind. Electron.*, vol. 16, no. 8, pp. 3304–3317, Aug. 2012.

[3] T. N. Do, T. Tjahjowidodo, M. W. S. Lau, T. Yamamoto, and S. J. Phee, "Hysteresis modeling and position control of tendon-sheath mechanism in flexible endoscopic systems," *Mechatronics*, vol. 24, no. 1, pp. 12–22, Feb. 2014.

[4] J. Cortes, "Discontinuous dynamical systems," *IEEE Control Syst. Mag.*, vol. 28, no. 3, pp. 36–73, Jun. 2008.

[5] M.-F. Danca, "Controlling chaos in discontinuous dynamical systems," *Chaos Solitons Fractals*, vol. 22, no. 3, pp. 605–612, Nov. 2004.

[6] H. K. Khalil, *Nonlinear Systems*, 3rd ed. Upper Saddle River, NJ, USA: Prentice-Hall, 2002.

[7] M. Jin, S. H. Kang, and P. H. Chang, "Robust compliant motion control of robot with nonlinear friction using time-delay estimation," *IEEE Trans. Ind. Electron.*, vol. 55, no. 1, pp. 258–269, Jan. 2008.

[8] Z. Li, C.-Y. Su, and X. Chen, "Modeling and inverse adaptive control of asymmetric hysteresis systems with applications to magnetostrictive actuator," *Control Eng. Pract.*, vol. 33, pp. 148–160, Dec. 2014.

[9] J. Lee *et al.*, "An experimental study on time delay control of actuation system of tilt rotor unmanned aerial vehicle," *Mechatronics*, vol. 22, no. 2, pp. 184–194, Mar. 2012.

[10] I. U. Ponce, Y. Orlov, L. T. Aguilar, and J. Álvarez, "Nonsmooth H_∞ synthesis of non-minimum-phase servo-systems with backlash," *Control Eng. Pract.*, vol. 46, pp. 77–84, Jan. 2016.

[11] B. Samadi and L. Rodrigues, "A sum of squares approach to back-stepping controller synthesis for piecewise affine and polynomial systems," *Int. J. Robust Nonlin. Control*, vol. 24, no. 16, pp. 2365–2387, Nov. 2014.

[12] F. Aghili and M. Namvar, "Adaptive control of manipulators using uncalibrated joint-torque sensing," *IEEE Trans. Robot.*, vol. 22, no. 4, pp. 854–860, Aug. 2006.

[13] W.-F. Xie, "Sliding-mode-observer-based adaptive control for servo actuator with friction," *IEEE Trans. Ind. Electron.*, vol. 54, no. 3, pp. 1517–1527, Jun. 2007.

[14] Q. Ling, Z. Yan, H. Shen, J. Li, and Y. Wang, "Robust switching control strategy for a transmission system with unknown backlash," *Math. Problems Eng.*, vol. 2014, pp. 1–8, Apr. 2014.

[15] M. Rakhshan, N. Vafamand, M. Shasadeghi, M. Dabbaghjamanesh, and A. Meeini, "Design of networked polynomial control systems with random delays: Sum of squares approach," *Int. J. Autom. Control*, vol. 10, no. 1, pp. 73–86, 2016.

[16] H. Moodi and M. Farrokhi, "Robust observer-based controller design for Takagi–Sugeno systems with nonlinear consequent parts," *Fuzzy Sets Syst.*, vol. 273, pp. 141–154, Aug. 2015.

[17] P. Tabarisaadi, M. M. Mardani, M. Shasadeghi, and B. Safarinejadian, "A sum-of-squares approach to consensus of nonlinear leader–follower multi-agent systems based on novel polynomial and fuzzy polynomial models," *J. Frankl. Inst.*, Oct. 2017, doi: 10.1016/j.jfranklin.2017.09.022.

[18] K. Tanaka, *Fuzzy Control Systems Design and Analysis: A Linear Matrix Inequality Approach*. New York, NY, USA: Wiley, 2001.

[19] J. Dong and G.-H. Yang, "Observer-based output feedback control for discrete-time T–S fuzzy systems with partly immeasurable premise variables," *IEEE Trans. Syst., Man, Cybern., Syst.*, vol. 47, no. 1, pp. 98–110, Jan. 2017.

[20] J. Dong and G.-H. Yang, "H_∞ filtering for continuous-time T–S fuzzy systems with partly immeasurable premise variables," *IEEE Trans. Syst. Man Cybern. Syst.*, vol. 47, no. 8, pp. 1931–1940, Aug. 2017.

[21] Q. Zhang, L. Qiao, B. Zhu, and H. Zhang, "Dissipativity analysis and synthesis for a class of T–S fuzzy descriptor systems," *IEEE Trans. Syst., Man, Cybern., Syst.*, vol. 47, no. 8, pp. 1774–1784, Aug. 2017.

[22] S. Beyhan, "Affine T–S fuzzy model-based estimation and control of Hindmarsh–Rose neuronal model," *IEEE Trans. Syst., Man, Cybern., Syst.*, vol. 47, no. 8, pp. 2342–2350, Aug. 2017.

[23] S. Wen, M. Z. Q. Chen, Z. Zeng, X. Yu, and T. Huang, "Fuzzy control for uncertain vehicle active suspension systems via dynamic sliding-mode approach," *IEEE Trans. Syst., Man, Cybern.*, vol. 47, no. 1, pp. 24–32, Jan. 2017.

[24] D. Saifia, M. Chadli, H. R. Karimi, and S. Labiod, "Fuzzy control for Electric Power Steering System with assist motor current input constraints," *J. Frankl. Inst.*, vol. 352, no. 2, pp. 562–576, Feb. 2015.

[25] X. Li, X.-P. Zhao, and J. Chen, "Controller design for electric power steering system using T–S fuzzy model approach," *Int. J. Autom. Comput.*, vol. 6, no. 2, pp. 198–203, May 2009.

[26] M.-F. Danca, "Continuous approximations of a class of piecewise continuous systems," *Int. J. Bifurcation Chaos*, vol. 25, no. 11, Oct. 2015, Art. no. 1550146.

[27] G. R. Arce, *Nonlinear Signal Processing: A Statistical Approach*. Hoboken, NJ, USA: Wiley, 2005.

[28] J. Na, Q. Chen, X. Ren, and Y. Guo, "Adaptive prescribed performance motion control of servo mechanisms with friction compensation," *IEEE Trans. Ind. Electron.*, vol. 61, no. 1, pp. 486–494, Jan. 2014.

[29] J. Bustamante, J. M. Quesada, and R. Martínez-Cruz, "Best one-sided L1 approximation to the Heaviside and sign functions," *J. Approx. Theory*, vol. 164, no. 6, pp. 791–802, Jun. 2012.

[30] S. M. Hashemi and H. Werner, "Gain-scheduled H_∞ control of a robotic manipulator with nonlinear joint friction," in *Proc. 1st Virtual Control Conf.*, Aalborg, Denmark, 2010, pp. 60–67.

[31] N. Vafamand, M. H. Asemani, and A. Khayatiyan, "A robust L1 controller design for continuous-time T–S systems with persistent bounded disturbance and actuator saturation," *Eng. Appl. Artif. Intell.*, vol. 56, pp. 212–221, Nov. 2016.

[32] N. Vafamand, M. H. Asemani, and A. Khayatian, "Robust L1 observer-based non-PDC controller design for persistent bounded disturbed T–S fuzzy systems," *IEEE Trans. Fuzzy Syst.*, to be published, doi: 10.1109/TFUZZ.2017.2724018.

[33] C.-S. Tseng, B.-S. Chen, and Y.-F. Li, "Robust fuzzy observer-based fuzzy control design for nonlinear systems with persistent bounded disturbances: A novel decoupled approach," *Fuzzy Sets Syst.*, vol. 160, no. 19, pp. 2824–2843, Oct. 2009.

[34] N. Vafamand and M. S. Sadeghi, "More relaxed non-quadratic stabilization conditions for T–S fuzzy control systems using LMI and GEVP," *Int. J. Control Autom. Syst.*, vol. 13, no. 4, pp. 995–1002, Aug. 2015.

[35] H. D. Tuan, P. Apkarian, T. Narikiyo, and Y. Yamamoto, "Parameterized linear matrix inequality techniques in fuzzy control system design," *IEEE Trans. Fuzzy Syst.*, vol. 9, no. 2, pp. 324–332, Apr. 2001.

[36] G. Tao and F. L. Lewis, Eds., *Adaptive Control of Nonsmooth Dynamic Systems*. London, U.K.: Springer, 2013.

[37] S. Tarbouriech, I. Queinnec, and C. Prieur, "Stability analysis and stabilization of systems with input backlash," *IEEE Trans. Autom. Control*, vol. 59, no. 2, pp. 488–494, Feb. 2014.

Authors' photographs and biographies not available at the time of publication.